Phase diagram of an Ising model with long-range frustrating interactions: A theoretical analysis

M. Grousson,[1] G. Tarjus,[1] and P. Viot[1,2]
[1]*Laboratoire de Physique Théorique des Liquides, Université Pierre et Marie Curie, 4 place Jussieu, 75252 Paris Cedex 05, France*
[2]*Laboratoire de Physique Théorique, Batiment 210, Université Paris–Sud, 91405 Orsay Cedex, France*
(Received 16 June 2000)

We present a theoretical study of the phase diagram of a frustrated Ising model with nearest-neighbor ferromagnetic interactions and long-range (Coulombic) antiferromagnetic interactions. For nonzero frustration, long-range ferromagnetic order is forbidden, and the ground state of the system consists of phases characterized by periodically modulated structures. At finite temperatures, the phase diagram is calculated within the mean-field approximation. Below the transition line that separates the disordered and the ordered phases, the frustration-temperature phase diagram displays an infinite number of ''flowers,'' each flower being made by an infinite number of modulated phases generated by structure combination branching processes. The specificities introduced by the long-range nature of the frustrating interaction and the limitation of the mean-field approach are finally discussed.

PACS number(s): 05.50.+q, 05.70.Fh, 64.60.Cn

I. INTRODUCTION

There are many physical examples in which a short-ranged tendency to order is opposed by a long-range frustrating interaction. In diblock copolymers formed by two mutually incompatible polymer chains attached to each other, the repulsive short-range forces between the two types of components tend to induce phase separation of the melt, but total segregation is forbidden by the covalent bonds that link the subchains together. A microphase separation transition occurs instead at low enough temperature, and the system then forms phases with a periodical modulation of structures rich in one component or the other, such as lamellar, hexagonal, or cubic phases [1,2]. In a similar way, self-assembly in water-oil-surfactant mixtures results from the competition between the short-range tendency of water and oil to phase separate and the stoichiometric constraints generated by the presence of surfactant molecules, constraints that act as the electroneutrality condition in a system of charged particles [3–5]. The same kind of physics also arises in quite different fields. For instance, stripe formation in doped antiferromagnets like cuprates has been ascribed to a frustrated electronic phase separation, by which a strong local tendency of the holes to phase separate into a hole-rich ''metallic'' phase and a hole-poor antiferromagnetic phase is prohibited by the long-range Coulombic repulsion between the holes [6,7]. A last example is provided by the structural or topological frustration in glass-forming liquids: the dramatic slowing down of the relaxation that leads to the glass formation has been interpreted as resulting from the presence of frustration-limited domains whose formation comes from the inability of the locally preferred arrangement of the molecules in the liquid to tile space periodically [8]; topological frustration may also lead to low-temperature defect-ordered phases, such as the Frank-Kasper [9] phases in bimetallic systems.

A coarse-grained description of the above-mentioned situations[1] involves lattice or continuum models with competing short-range and Coulombic interactions. The purpose of the present work is to study the phase diagram of such a model, namely the Coulomb frustrated Ising ferromagnet in which Ising spins placed on a three-dimensional cubic lattice interact via both nearest-neighbor ferromagnetic couplings and long-range Coulomb-like antiferromagnetic terms. The model is introduced in more detail in Sec. II and its ground state as a function of the frustration parameter, i.e., of the ratio of the antiferromagnetic coupling strength over the ferromagnetic one, is studied in Sec. III. In Sec. IV, we investigate the finite-temperature phase diagram in the mean-field approximation. Finally, the effect of the long-range nature of the frustrating forces (when comparing to the phase behavior of the prototypical model with competing, but short-ranged interactions, the axial next-nearest-neighbor Ising (ANNNI) model [10–12]), as well as the limitations of the mean-field approach are discussed in Sec. V.

II. THE COULOMB FRUSTRATED ISING FERROMAGNET

The model is described by the Hamiltonian

$$H=-J\sum_{\langle ij\rangle} S_iS_j+\frac{Q}{2}\sum_{i\neq j} v(\mathbf{r}_{ij})S_iS_j\,, \tag{1}$$

where, $J,Q>0$ are the ferromagnetic and antiferromagnetic coupling strengths, $S_i=\pm 1$ are Ising spin variables placed on the sites of a three-dimensional cubic lattice, $\langle ij\rangle$ denotes a sum restricted to nearest neighbors, $\mathbf{r}_{ij}$ is the vector joining sites i and j, and $v(\mathbf{r})$ represents a Coulomb-like interaction term with $v(\mathbf{r})\sim 1/|\mathbf{r}|$ when $|\mathbf{r}|\to\infty$. (Throughout the paper, the lattice spacing is taken as the unit length.) The above

[1]Additional examples include cross-linked polymer mixtures, interpenetrating networks, and ultrathin films.

Hamiltonian is essentially the ''hard-spin'' version of the coarse-grained free-energy functional derived by Ohta and Kawasaki [13] for symmetric diblock copolymer systems, with $S_i = \pm 1$ characterizing whether the system is locally rich in one type of monomer or another, J/k_BT playing the role of the Flory-Huggins interaction parameter, and Q/J being proportional to $1/N^2$, where N is the overall degree of polymerization of a copolymer.

In addition to considering the true Coulombic term, $v(\mathbf{r}) = 1/|\mathbf{r}|$, we have also studied, for mathematical convenience in the analytical treatment, an expression of $v(\mathbf{r})$ in terms of the lattice Green's function that satisfies the Poisson equation on the three-dimensional cubic lattice. In the latter case, $v(\mathbf{r})$ is then simply given, up to a multiplying factor of 4π, as the inverse Fourier transform of the inverse lattice Laplacian,

$$v(\mathbf{r}) = \frac{4\pi}{N} \sum_{\mathbf{k}} \frac{\exp(-i\mathbf{k}\cdot\mathbf{r})}{2\sum_{\alpha=x,y,z}[1-\cos(k_\alpha)]}, \tag{2}$$

where N is the number of lattice sites and the sum over $\mathbf{k} = (k_x, k_y, k_z)$ is restricted to the first Brillouin zone. For large $|\mathbf{r}|$ the lattice Green's function behaves as $1/(4\pi|\mathbf{r}|)$, so that the expression in Eq. (2) has the proper asymptotic behavior. In practice, even at the next-neighbor distance, the difference between the true Coulombic form and Eq. (2) is very small [14]. One has, however, to be careful about two points. The first one is that the $v(\mathbf{r})$ defined in Eq. (2) has a nonzero, finite value at $\mathbf{r}=0$, $v(\mathbf{0}) = 0.252\,731\,009\,86\ldots$, a value that must of course be excluded when considering the Hamiltonian in Eq. (1).[2] For instance, Eq. (1) when expressed in Fourier space, can be written as

$$H = \frac{J}{2} \sum_{\mathbf{k}} \hat{V}(\mathbf{k}) |\hat{S}(\mathbf{k})|^2, \tag{3}$$

where

$$\hat{V}(\mathbf{k}) = -2\sum_{\alpha=x,y,z}\cos(k_\alpha) + \frac{4\pi Q}{J} \times \left[\frac{1}{2\sum_{\alpha=x,y,z}[1-\cos(k_\alpha)]} - v(\mathbf{0}) \right] \tag{4}$$

and $\hat{S}(\mathbf{k})$ is the lattice Fourier transform of the Ising spin variable S_i. To assess the quantitative difference between the Coulombic form and that involving the lattice Green's function, we have calculated the energy of the system in several periodic configurations of the spins. For periodic lamellar patterns of large width m, the difference is negligible, but it increases when m decreases. For a Néel antiferromagnetic state, the Coulombic energy is related to the Madelung constant and is equal to $-0.873\,782\ldots$, whereas the lattice Green's-function expression gives $-1.064\,356\,992$.

The second point worth mentioning is that the $v(\mathbf{r})$ expressed in terms of the lattice Green's function has the same discrete symmetry as the nearest-neighbor ferromagnetic interaction, whereas the true Coulombic form has continuous rotational symmetry instead. The consequences are negligible for the ground-state and for mean-field analyses, but may become important for the finite-temperature behavior of the system in other approximations [17].

III. PHASE DIAGRAM AT ZERO TEMPERATURE

In the absence of the antiferromagnetic interaction ($Q = 0$) the model reduces to the standard Ising ferromagnet, and the ground state of the system is obtained when all spins are aligned in a ferromagnetic state. Oppositely, when the ferromagnetic interaction is set to zero ($J = 0$), the model is equivalent to a Coulomb lattice gas and the ground-state of the system is a Néel antiferromagnetic state. When $Q \neq 0$, the Coulombic interaction prevents the existence of a ferromagnetic phase, and in the thermodynamic limit, the total magnetization (charge) is constrained to be zero. Instead, phases with modulated order, i.e., with periodic patterns of ''up'' and ''down'' spins subject to the constraint of zero magnetization, are formed. We have studied these phases both analytically with the long-range interactions modeled by the lattice Green's function and numerically with the true Coulombic form.

For small values of the frustration parameter Q/J, the ground state consists of lamellar phases in which parallel planes of ferromagnetically aligned spins form a periodic structure along the orthogonal direction. The system in such a state can be mapped onto a finite one-dimensional system of length $2m$, where m denotes the width of the lamellae [18,19].

The short-range ferromagnetic contribution to the energy per spin of a lamellar phase can be readily calculated, and one gets

$$E_{SR} = -J\left(3 - \frac{2}{m}\right). \tag{5}$$

The Coulombic energy due to the long-range competing forces can be calculated in reciprocal space by using the expression in terms of the inverse lattice Laplacian (see Sec. II). For a lamellar phase of period $2m$, the wave vectors to be considered have only one nonzero component that takes the values $k = \pi(2n+1)/m$ with $0 \leqslant n < m-1$. Correspondingly, the lattice Fourier transform of the Ising spin variable, $\hat{S}(\mathbf{k}) = (1/\sqrt{N})\Sigma_{i=1}^{N} S_i \exp(i\mathbf{k}\cdot\mathbf{r}_i)$, where N is the total number of lattice site, has its modulus given by

$$|\hat{S}(\mathbf{k})| = |\hat{S}(k)| = \frac{\sqrt{N}}{m\sin(k/2)}. \tag{6}$$

Using then the identities

$$\sum_{n=0}^{m-1} \frac{1}{\sin[\pi(2n+1/(2m)]^2} = m^2, \tag{7}$$

[2]The correction term involving $v(\mathbf{0})$ in Eq. (4) has been omitted in previous papers [15,16], but it leads only to very small corrections when the parameter Q/J is small.

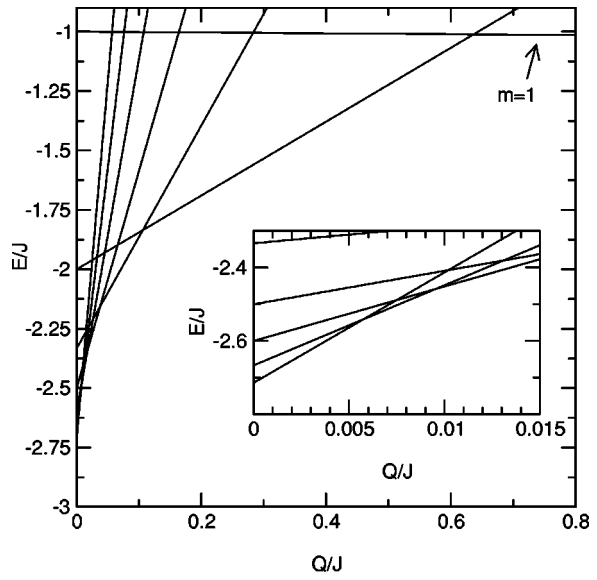

FIG. 1. Ground-state energy of the lamellar phases with $m=1,2,\ldots,7$ as a function of the frustration parameter Q/J for the inverse lattice Laplacian expression of $v(\mathbf{r})$. When Q/J goes to zero, the period of the lamellar phases increases. The inset zooms in on the region of vanishing frustration parameters, which corresponds to the lower left region of the figure.

$$\sum_{n=0}^{m-1} \frac{1}{\sin[(\pi(2n+1/(2m)]^4} = \frac{m^4}{3} + \frac{2m^2}{3}, \tag{8}$$

one finds that the sum rule $\Sigma_k |\hat{S}(k)|^2 = N$ is properly satisfied and that the Coulombic energy per site, E_c, is equal to

$$E_c = Q\left[\sum_{n=0}^{m-1} \frac{\pi}{2\sin[\pi(2n+1)/(2m)]^4} - 2\pi v(0)\right] \tag{9}$$

$$= Q\left[\frac{\pi m^2}{6} + \pi\left[\tfrac{1}{3} - 2v(0)\right]\right]. \tag{10}$$

In Appendix A, we show that the same expression for the Coulombic energy is obtained when performing the calculation in real space with an effective one-dimensional potential; this latter includes a convergence factor that helps handling conditionally convergent sums appearing as a result of the long-range nature of the forces and that is taken to zero at the end of the calculation. It is worth mentioning that the above calculation in reciprocal space implicitly assumes that the contribution from the $k=0$ term is zero; physically, this means that the periodic system is embedded in a medium with infinite dielectric constant. (For a more detailed discussion, see Ref [20].) Since for simulations on ionic systems, a similar choice is generally adopted [20], both numerical and analytical calculations for our model have been performed using such metallic boundary conditions.

Figure 1 shows the total energy per spin, E/J, which is the sum of the two contributions in Eqs. (5) and (10) for the inverse lattice Laplacian expression, as a function of Q/J for small values of the frustration parameter Q/J. (The plot for the true Coulombic potential is very similar.) The slope of each straight line corresponds to the Coulombic energy and the intercept with the y axis corresponds to the short-range ferromagnetic energy. For a given frustration parameter Q/J, the ground state is given by the straight line that has the smallest energy. When $Q/J \to 0$, the ground state consists of lamellar phases whose period becomes larger and larger and whose range of stability decreases. The values of Q/J corresponding to transitions between two successive ground-state structures are obtained by solving the equation $E(m) = E(m+1)$. Therefore, when Q/J goes to zero, m is asymptotically given by

$$m \sim (Q/J)^{-1/3}, \tag{11}$$

a behavior that is analogous to that observed for lamellar phases of diblock copolymer systems at low temperature in the so-called strong segregation limit [13]. (Recall that Q/J plays the role of $1/N^2$ where N is the total number of segments on a polymer.) Note that for a large width m, the difference between Eq. (10) and the value obtained from the true Coulombic term is only weakly varying with m and can be taken as a constant, so that Eq. (11) also provides a very accurate estimate both for the sequence of lamellar phases and for the transition values of Q/J for the true Coulombic potential.

When Q/J increases, the period of the lamellar phases decreases until one reaches $m=1$ for $Q/J=0.637$. For a region of the frustration parameter between 0.637 and 1.800, this lamellar phase is then the most stable phase. In a narrow interval between $Q/J=1.800$ and $Q/J=2.122$ there is a cascade of phases $(1\times m_2\times\infty)$, with m_2 decreasing until $m_2=2$ as the frustration parameter increases [see Fig. 2(a)]. For $2.122<Q/J<3.820$, the stable phase is $(1\times 2\times\infty)$. Note that tubular phases of the type $(m_1\times m_2\times\infty)$ with both m_1 and $m_2>1$ are never stable. For $3.820<Q/J<6.237$, the ground state is a $1\times 1\times\infty$ tube. In another interval $6.237<Q/J<6.611$, the system loses translational invariance in the third direction, and one observes a cascade of orthorhombic phases $(1\times 1\times m_3)$, with m_3 decreasing as the frustration increases until $m_3=2$. Between 6.611 and 9.549, the stable phase is $(1\times 1\times 2)$. For $Q/J>9.549$, the ground state is the standard Néel state $(1\times 1\times 1)$ [see Fig. 3(a)]. It is noticeable that periodic structures of the type $(m_1\times m_2\times m_3)$ with $m_1, m_2, m_3>1$ and at least one of the m_α's finite always have higher energies than those of the sequences $(m_1\times\infty\times\infty)$, $(\infty\times m_2\times\infty)$, $(\infty\times\infty\times m_3)$, whatever the value of the frustration parameter (see Appendix B).

The same analysis can be repeated with $v(\mathbf{r})$ given by the true Coulomb interaction. The exact same sequence of ground states as before is obtained, but the values of the frustration parameter at the transition points are somewhat shifted: For instance, the lamellar phase $m=1$ is the most stable phase when $0.627<Q/J<5.21$, the cascade of ''tubular'' phases $(1\times m_2\times\infty)$ occurs around $Q/J=5.22$, and $(1\times 2\times\infty)$ is stable for $5.23<Q/J<6.17$ [see Fig. 2(b)]. The cascade of ''orthorhombic'' phases $(1\times 1\times m_3)$, with $m_3>1$, appears around $Q/J=14.63$ [see Fig. 3(b)]. The standard Néel state is stable for $Q/J>15.33$. It is worth mentioning that the counterparts of the lamellar, tubular, and orthorhombic phases in diblock copolymer systems [2] [systems that are described at a coarse-grained level by the scalar field theory associated with the Hamiltonian in Eq. (1)] are the lamellar, columnar, and cubic phases, respectively.

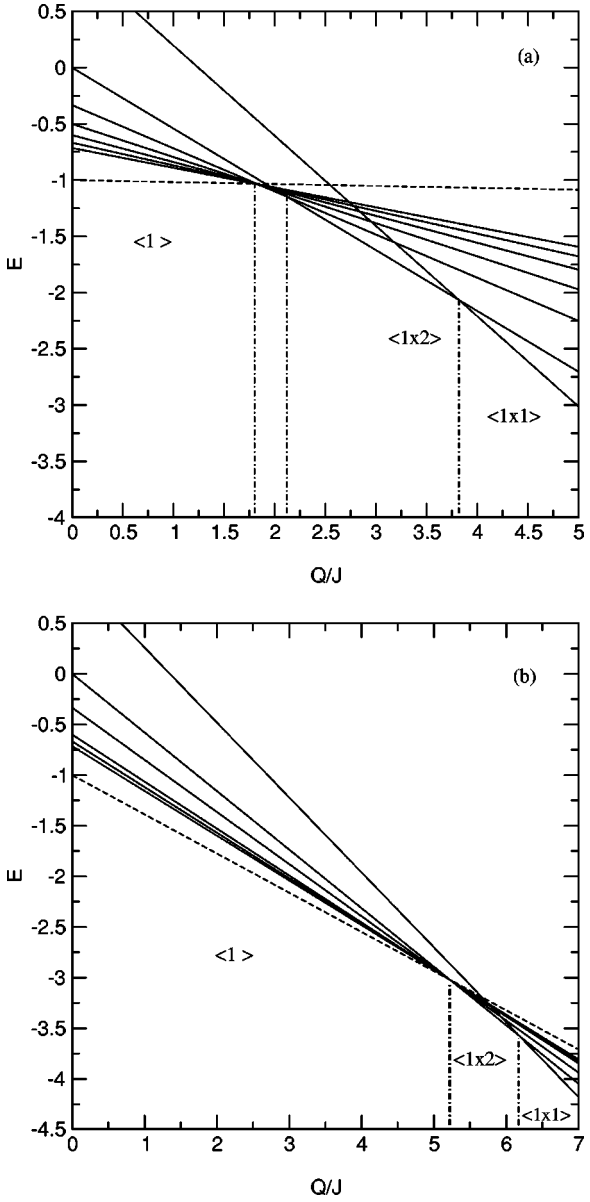

FIG. 2. Ground-state energy of the tubular phases with $m_2=1,2,\ldots,7$ (full lines) and $m_2=\infty$ (dashed line) as a function of the frustration parameter Q/J. (a) For the inverse lattice Laplacian expression, the tubular phases, $(1\times m_2\times\infty)$ with $m_2>1$, are stable for frustration parameters $1.800<Q/J<3.820$. (b) For the true Coulombic potential, the tubular phases are stable for $5.21<Q/J<6.17$. $\langle 1\rangle$, $\langle 1\times 2\rangle$ and $\langle 1\times 1\rangle$ are short-hand notations for $\langle 1\times\infty\times\infty\rangle$, $\langle 1\times 2\times\infty\rangle$, and $\langle 1\times 1\times\infty\rangle$, respectively. The vertical dot-dashed lines are visual guides for denoting the stability region of the phases.

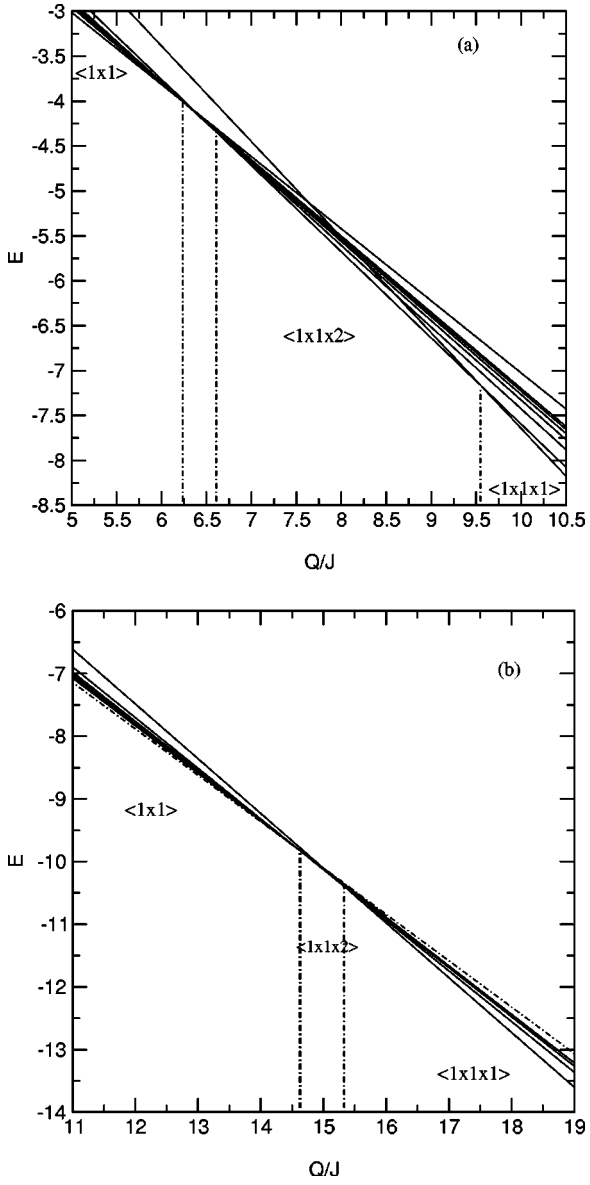

FIG. 3. Energy of the orthorhombic phases with $m_3=1,2,\ldots,7$ as a function of the frustration parameter Q/J. (a) For the inverse lattice Laplacian expression, the orthorhombic phases $(1\times 1\times m_3)$ with $m_3>1$ are stable for frustration parameters $6.237<Q<9.549$. (b) For the true Coulombic potential, the orthorhombic phases are for $14.63<Q/J<15.33$. $\langle 1\times 1\rangle$ is a short-hand notation for $\langle 1\times 1\times\infty\rangle$. The vertical dot-dashed lines are visual guides for denoting the stability region of the phases.

In the region of stability of the lamellar phases, we have also investigated if more complex structures involving several one-dimensional modulations of ferromagnetically ordered layers could be present and if multiphase transition points at which more than simply two phases coexist could occur. For both questions, the answer is negative. As an example, we give in Appendix C the analytical expressions for the energy of the mixed lamellar phases that are formed by mixing lamellae of width $m=1$ and lamellae of width $m=2$ with some given periodic modulation. The simplest of such phases, which following the notation used by Selke and Fisher in their study of the axial next-nearest-neighbor Ising (ANNNI) model [11] we denote $\langle 1^n 2^p\rangle$, consists of a periodic repetition of a fundamental pattern formed by a succession of n lamellae of width 1 followed by p lamellae of width 2. (When $n=0$, one recovers the simple lamellar phase of width 2, denoted $\langle 2\rangle$, and when $p=0$, one recovers the simple lamellar phase of width 1, denoted $\langle 1\rangle$.) It is easy to check that such mixed lamellar phases are never stable at zero temperature. In particular, they have a (strictly) higher energy than the pure lamellar phases at the zero-temperature transition point between the $\langle 1\rangle$ and the $\langle 2\rangle$ phases, at $Q/J=2/\pi$, so that this latter is a simple two-phase coexistence point. This conclusion remains unchanged when one consid-

ers even more complex mixed lamellar phases, such as $\langle 1^{n_1}2^{p_1}1^{n_2}2^{p_2}\ldots 1^{n_s}2^{p_s}\rangle$, with n_α, p_α integers for $\alpha = 1,2,\ldots s$, whose fundamental period is formed by n_1 one-layer lamellae followed by p_1 two-layer lamellae, then by n_2 one-layer lamellae, and by p_2 two-layer lamellae, etc., two successive lamellae being composed of spins of opposite signs. We have also studied one-dimensional quasi crystalline arrangements of lamellae: by using binary substitution rules, [21] we have built quasi periodic structures by iteration, but we have always found (numerically) that their energy is higher than that of the pure lamellar phases. Note finally that from the calculation of the energy of the mixed lamellar phases at zero temperature, one can also study the change of energy induced by adding defects in the pure lamellar phase $\langle 2\rangle$. As shown in Appendix C, adding defects always costs energy, the dominant effect being the increase in the short-range energy. The same analysis, leading to a similar conclusion, can be repeated for the whole range $0 < Q/J < 0.637$ over which lamellar phases are favored.

IV. MEAN-FIELD THEORY

To describe phases with a spatial modulation of the magnetization, we consider a local mean-field approximation. If $m_i = \langle S_i\rangle$ denotes the local magnetization at site i, and $\hat{m}(k)$ its lattice Fourier transform, the mean-field free energy F_{mf} is given by

$$\frac{\beta F_{mf}}{N} = -\frac{\beta J}{2N}\sum_{\mathbf{k}\neq 0}\hat{V}(\mathbf{k})|\hat{m}(\mathbf{k})|^2 - \frac{1}{N}\sum_i \ln[2\cosh(\beta H_i)], \tag{12}$$

where $\beta = 1/k_B T$ and the effective field on site i, H_i, is equal to $-J\Sigma_{j\neq i}V_{ij}m_j$, or in Fourier transformed space,

$$\hat{H}(\mathbf{k}) = -J\hat{V}(\mathbf{k})\hat{m}(\mathbf{k}). \tag{13}$$

Minimization of the free energy with respect to the local magnetizations leads to the self-consistent set of equations:

$$m_i = \tanh(\beta H_i), \tag{14}$$

for each lattice site. One must then solve the coupled equations, Eqs. (13) and (14), simultaneously, and subsequently insert the solution in the expression of the free energy, Eq. (12). One finally searches for the configuration of the m_i's that leads to the deepest minimum of the free energy for a given temperature and a given value of the frustration parameter.

To simplify the notation in the rest of the paper, units of temperature, energy, etc. will be chosen such that $k_B = J = 1$.

A. Order-disorder transition line

Close to the transition between the disordered and the ordered phases, the magnetizations m_i are small and Eq. (14) can be linearized,

$$m_i \approx \frac{H_i}{T}. \tag{15}$$

For a given value of the frustration parameter, the critical temperature $T_c(Q)$ is then given by

$$T_c(Q) = -\min_{\mathbf{k}}\hat{V}(\mathbf{k}), \tag{16}$$

where the minimum of $\hat{V}(\mathbf{k})$ is attained for a set of nonzero wave vectors $\{\mathbf{k}_c(Q)\}$ that characterize the ordering at $T_c(Q)$. For the inverse lattice Laplacian expression of the long-range frustrating interaction, the $\mathbf{k}_c(Q)$'s vary continuously with Q as follows:

$$\mathbf{k}_c = (\pm\arccos(1-\sqrt{\pi Q}),0,0) \quad \text{for } 0\leqslant Q < 4/\pi, \tag{17}$$

$$\mathbf{k}_c = (\pi, \pm\arccos(3-\sqrt{\pi Q}),0) \quad \text{for } 4/\pi \leqslant Q < 16/\pi, \tag{18}$$

$$\mathbf{k}_c = (\pi,\pi,\pm\arccos(5-\sqrt{\pi Q})) \quad \text{for } 16/\pi \leqslant Q < 36/\pi, \tag{19}$$

$$\mathbf{k}_c = (\pi,\pi,\pi) \quad \text{for } 36/\pi \leqslant Q. \tag{20}$$

One should of course add all vectors obtained by permuting the x,y,z coordinates in Eqs. (17)–(20). The above ordering wave-vectors correspond, respectively, to lamellar [Eq. (17)], tubular [Eq. (18)], orthorhombic [Eq. (19)], and cubic or Néel [Eq. (20)] phases. When $Q\to 0$ the ordering wave vector of the lamellar structure goes as $Q^{1/4}$, which is analogous to the result predicted for diblock copolymer systems in the weak-segregation limit [1,22].

The corresponding critical temperature $T_c(Q)$ is then given by (recall that both T and Q are expressed in units of J)

$$T_c(Q) = 6 - 4\sqrt{\pi Q} + 4\pi Q v(0) \quad \text{for } 0\leqslant Q \leqslant 36/\pi, \tag{21}$$

$$T_c(Q) = -6 + 4\pi Q\left(v(0) - \frac{1}{12}\right) \quad \text{for } 36/\pi \leqslant Q. \tag{22}$$

The mean-field approximation gives a line of second-order phase transition from the disordered to the modulated phases, with $T_c(Q)$ first decreasing with Q, reaching a minimum for $Q_{min} = 1/[4\pi v(0)^2] = 1.245871$ at $T_c(Q_{min}) = 6 - 1/v(0)$ and then increasing again for finally reaching a regime of linear increase with Q when $Q \geqslant 36/\pi$. It is worth noting that the term $4\pi Q v(0)$ is important for large frustration: indeed, since $v(0) > 1/6$, it allows one to obtain a positive critical temperature for all Q's. [In general, $v(0)$ should be larger than the inverse of the number of nearest neighbors on the lattice, e.g., 6 on a simple cubic lattice.] For vanishingly small frustration, the critical temperature goes continuously to T_c^0, the critical temperature of the pure Ising ferromagnet.

B. Structure combination branching processes

At zero temperature, we showed that the system exists in pure modulated phases, whose modulation is commensurate with the underlying lattice. At the transition between the modulated and disordered phases, we have just seen that the ordering wave vector varies continuously with the frustration parameter, hence indicating that a succession of incommen-

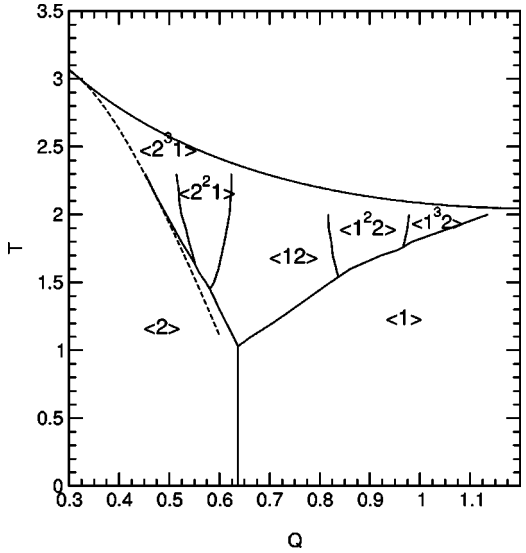

FIG. 4. Mean-field phase diagram: structure combination branching processes occurring at finite temperatures for a region of frustration parameter where the ground states consist of $\langle 1\rangle$ and $\langle 2\rangle$ phases. The dashed line corresponds to the soliton-approach prediction for the (upper) stability of the $\langle 2\rangle$ phase. The units are chosen such that $k_B=J=1$.

surate modulated phases is observed along the critical line. As the temperature increases from $T=0$ to $T_c(Q)$, one expects a cascade of ordered phases with commensurate spatial modulations of increasing complexity until a point is reached at which incommensurate phases appear; this is what is observed for instance in the much studied axial next-nearest neighbor Ising model [12], in which the cascade of phases is produced by ''structure combination branching processes'' [12]. To illustrate how such branching processes proceed, we consider first the low-temperature region of the phase diagram in which the simplest modulated phases, the $\langle 1\rangle$ and $\langle 2\rangle$ lamellar phases, are stable (see Fig. 4). Equations (13) and (14) must now be solved beyond the linear approximation. The $\langle 1\rangle$ phase corresponds to an alternate configuration of layers of up and down spins, with $m_i=m_1(-1)^i$, which implies that the wave vector characterizing the modulation has only one nonzero component equal to $k=\pi$. Using Eq. (13) and Eq. (14), one gets

$$m_1=\tanh\left[\frac{m_1}{T}[2-\pi Q+4\pi Q v(0)]\right], \tag{23}$$

which has a nonzero solution when

$$T<2-\pi Q+4\pi Q v(0). \tag{24}$$

From Eq. (12), the corresponding free energy is obtained as

$$\frac{F_{\langle 1\rangle}}{N}=\left(1-\frac{\pi Q}{2}+2\pi Q v(0)\right)m_1^2 - T\ln\left[2\cosh\left(\frac{m_1}{T}[2-\pi Q+4\pi Q v(0)]\right)\right]. \tag{25}$$

The $\langle 2\rangle$ phase corresponds to an alternate sequence of pairs of ferromagnetically ordered layers and is characterized by a wave vector whose only nonzero component is $k=\pi/2$. The corresponding order parameter m_2 satisfies the following equation:

$$\frac{\sqrt{2}}{2}m_2=\tanh\left[\frac{\sqrt{2}m_2}{T}[2-\pi Q+2\pi Q v(0)]\right], \tag{26}$$

which has a nonzero solution when

$$T<2-\pi Q+2\pi Q v(0). \tag{27}$$

The associated free energy is

$$\frac{F_{\langle 2\rangle}}{N}=\left(1-\frac{\pi Q}{2}+\pi Q v(0)\right)m_2^2 - T\ln\left[2\cosh\left(\frac{m_2\sqrt{2}}{T}[2-\pi Q+2\pi Q v(0)]\right)\right]. \tag{28}$$

The line of first-order transition at which the two phases coexist is defined by $F_{\langle 1\rangle}=F_{\langle 2\rangle}$. In the $T-Q$ phase diagram, this line is almost vertical with $Q\simeq 2/\pi$. As we have already stressed, no mixed phases coexist with the $\langle 1\rangle$ and $\langle 2\rangle$ phases at $T=0$ and $Q=2/\pi$. However, the mixed $\langle 12\rangle$ phase may become more stable at a nonzero temperature. This phase is characterized by the modulation $m_i=(2\sqrt{3}/3)m_{12}\cos(2\pi i/3+\pi/2)$, with the order parameter m_{12} determined through the self-consistent equation

$$m_{12}=\tanh\left[\frac{m_{12}}{T}\left(3-\frac{4\pi}{3}Q+4\pi Q v(0)\right)\right], \tag{29}$$

which has a nonzero solution for

$$T<3-\frac{4\pi}{3}Q+4\pi Q v(0). \tag{30}$$

The corresponding free energy is given by

$$\frac{F_{\langle 12\rangle}}{N}=\frac{1}{3}\left(3-\frac{4\pi Q}{3}-\pi Q v(0)\right)m_{12}^2 - \frac{2T}{3}\ln\left\{2\cosh\left[\frac{m_{12}}{T}\left(3-\frac{4\pi}{3}Q+4\pi Q v(0)\right)\right]\right\}. \tag{31}$$

Comparing now the free energy of the three phases, $\langle 1\rangle$, $\langle 2\rangle$, $\langle 12\rangle$, one can show that the $\langle 12\rangle$ phase becomes more stable than the other two in a wedge above a branching point at $T_b=1.03$ and $Q=0.63$, at which the three phases coexist. This represents the first step of a structure combination branching process by which two adjacent phases, here $\langle 1\rangle$ and $\langle 2\rangle$, get separated above a given branching point at finite temperature by a phase corresponding to the simplest combination structure, here the $\langle 12\rangle$ phase. A careful examination of the thermodynamic quantities shows that the entropy of the $\langle 12\rangle$ phase increases more rapidly with temperature than that of the $\langle 1\rangle$ and $\langle 2\rangle$ phases; although it has an

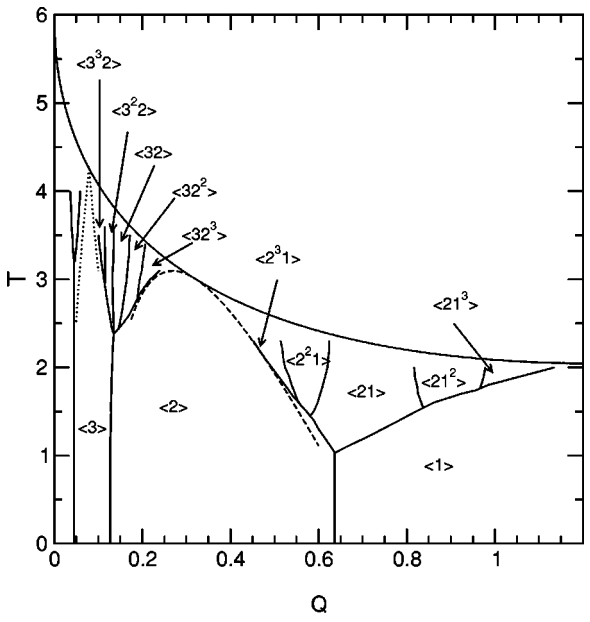

FIG. 5. Mean-field phase diagram: a (partial) view of the infinite sequence of ''flowers'' of complex modulated phases appearing at finite temperatures for the range of the frustration parameter where the ground states are lamellar phases. The dashed and dotted lines correspond to the soliton-approach prediction for the (upper) stability of the $\langle 2\rangle$ and $\langle 3\rangle$ phases, respectively. The units are chosen such that $k_B=J=1$.

unfavorable energy contribution, the $\langle 12\rangle$ phase becomes thermodynamically stable when the temperature becomes high enough ($T_b=1.03$). Moreover, for all temperatures between $T=0$ and T_b, both the entropy and the energy of the $\langle 1\rangle$ and $\langle 2\rangle$ phases are identical along the coexistence line between the two phases.

To study in more detail the branching processes, one can no longer rely on explicit analytical calculations as done above, because they become rapidly intractable. To obtain the phase diagram in a more systematic way, the mean-field equations, Eqs. (12)–(14), can be solved iteratively for finite lattices with periodic boundary conditions. The thermodynamically stable solution corresponds to that with the smallest free energy. For each temperature it is assumed that the spin structure repeats itself after N layers (only commensurate lamellar structures are considered). The iterative procedure converges whenever the initial configuration is not too far from the equilibrium one. The iterative sequence is as follows. The effective fields H_i are calculated from the set of initial magnetizations $\{m_i^0\}$ via Eq. (14). One computes the Fourier transform of the fields H_i, and using Eq. (13) yields then a new set of magnetizations $\{m_i^1\}$ that is used as the input for the next iteration. The calculation should be performed for various values of N for examining many different commensurate structures. We have carried out the calculation for N up to 16. The phases with large-N periodicities, like in the ANNNI phase diagram [12], are only stable in a small neighborhood of the critical line. Therefore, the most of the phase diagram, except in the region close to the critical line, can be drawn by considering simple commensurate wave vectors.

The results are shown in Figs. 4 and 5. Figure 4 illustrates the structure combination process in the region between the $\langle 1\rangle$ and $\langle 2\rangle$ phases. The $\langle 12\rangle$ and $\langle 1\rangle$ phases are separated by the $\langle 1^2 2\rangle$ phase, which itself is separated at higher temperature from the $\langle 1\rangle$ phase by the $\langle 1^3 2\rangle$ phase, and so on, until one presumably reaches an accumulation point of the branching process along the transition line above which the $\langle 1\rangle$ phase melts. Beyond this accumulation point corresponding to a sequence of $\langle 1^n 2\rangle$ phases when $n\to\infty$, devil's staircases and incommensurate phases are expected [12]. Figure 5 provides a broader picture of the phase diagram in the region where the modulated phases are lamellar: the phase diagram appears as a succession of flowers of complex modulated phases, separated by regions in which the pure lamellar phases $\langle 1\rangle$,$\langle 2\rangle$, etc., are stable; the flowers get closer and closer when the frustration decreases. Note that the first branching point at which the simplest mixed phase appears is always at a nonzero temperature.

C. Soliton approach

At high enough temperature, near the critical line, the modulated phases are incommensurate, since we saw in Sec. IV A that the ordering wave vector varies continuously with frustration. More insight in the phase behavior can then be provided by employing the soliton approach developed by Bak and co-workers [23,24]. More precisely, this approach allows one to study analytically the melting of a commensurate phase to incommensurate phases by focusing on the behavior of the domain walls that separate commensurate regions, domain walls that can be considered as ''solitons.'' In the following, we use the soliton method to investigate the stability of commensurate phases at high temperature.

In the vicinity of the (upper) melting line of the $\langle 2\rangle$ phase, one can expand the mean-field equations in the appropriate order variables, which leads to the following free-energy functional:

$$\frac{F}{N}=-\frac{1}{2}\sum_{\mathbf{k}}\left(\hat{V}(\mathbf{k})+\frac{1}{\beta}\right)|\hat{m}_{\mathbf{k}}|^2+\frac{T}{12}\times\sum_{\boldsymbol{\tau}}\sum_{\mathbf{k}_1,\ldots,\mathbf{k}_4}\delta(\mathbf{k}_1+\mathbf{k}_2+\mathbf{k}_3+\mathbf{k}_4-\boldsymbol{\tau})\hat{m}_{\mathbf{k}_1}\hat{m}_{\mathbf{k}_2}\hat{m}_{\mathbf{k}_3}\hat{m}_{\mathbf{k}_4}+\frac{T}{30}\sum_{\boldsymbol{\tau}}\sum_{\mathbf{k}_1,\ldots,\mathbf{k}_6}\delta(\mathbf{k}_1+\mathbf{k}_2+\mathbf{k}_3+\mathbf{k}_4+\mathbf{k}_5+\mathbf{k}_6-\boldsymbol{\tau})\times\hat{m}_{\mathbf{k}_1}\hat{m}_{\mathbf{k}_2}\hat{m}_{\mathbf{k}_3}\hat{m}_{\mathbf{k}_4}\hat{m}_{\mathbf{k}_5}\hat{m}_{\mathbf{k}_6}+\cdots, \tag{32}$$

where a constant term has been discarded and $\boldsymbol{\tau}$ is a reciprocal-lattice vector. The above expression, Eq. (32), contains both regular and ''umklapp'' terms; these latter, represented by the second and third contributions in the right-hand side of Eq. (32), correspond to terms in which the sum of the wave vectors is equal to a reciprocal-lattice vector, i.e., they keep track of the underlying lattice structure and are responsible for the stability of the commensurate phases.

For studying the stability of the $\langle 2\rangle$ phase near the critical line, we consider wave vectors that are close to the ordering wave vector $k_{\pi/2}=(\pi/2,0,0)$ with small fluctuations q_x in the direction of the modulation, here along the x axis, and $\mathbf{q}_\perp$ in the perpendicular layer. For the present case, it is sufficient

to truncate Eq. (32) after the fourth order [23], and after expanding the interaction term to second order in the fluctuations, the free-energy functional can be rewritten as

$$\frac{F}{N}=-\frac{1}{2}\sum_{\mathbf{q}=q_x,\mathbf{q}_\perp}(r+aq_x+cq_x^2+c'\mathbf{q}_\perp^2)|\hat{m}_{\mathbf{k}_{\pi/2}+\mathbf{q}}|^2$$
$$+T\sum_{\mathbf{q}_1\mathbf{q}_2\mathbf{q}_3\mathbf{q}_4}\delta(\mathbf{k}_1+\mathbf{k}_2+\mathbf{k}_3+\mathbf{k}_4)$$
$$\times[\tfrac{1}{2}\hat{m}_{\mathbf{k}_{\pi/2}+\mathbf{q}_1}\hat{m}_{\mathbf{k}_{\pi/2}+\mathbf{q}_2}\hat{m}_{-\mathbf{k}_{\pi/2}+\mathbf{q}_3}\hat{m}_{-\mathbf{k}_{\pi/2}+\mathbf{q}_4}$$
$$+\tfrac{1}{12}(\hat{m}_{\mathbf{k}_{\pi/2}+\mathbf{q}_1}\hat{m}_{\mathbf{k}_{\pi/2}+\mathbf{q}_2}\hat{m}_{\mathbf{k}_{\pi/2}+\mathbf{q}_3}\hat{m}_{\mathbf{k}_{\pi/2}+\mathbf{q}_4}$$
$$+\hat{m}_{-\mathbf{k}_{\pi/2}+\mathbf{q}_1}\hat{m}_{-\mathbf{k}_{\pi/2}+\mathbf{q}_2}\hat{m}_{-\mathbf{k}_{\pi/2}+\mathbf{q}_3}\hat{m}_{-\mathbf{k}_{\pi/2}+\mathbf{q}_4})], \quad (33)$$

where $r=T-4+2\pi Q-4\pi Q v(0)\leqslant 0$, $a=2-2\pi Q$, $c=2\pi Q$, and $c'=-\pi Q+1$. Now introducing two continuous order parameters,

$$m_+(\mathbf{r})=\sqrt{2}\int\frac{d^3q}{(2\pi)^3}\exp(i\mathbf{q}\cdot\mathbf{r})\hat{m}_{\mathbf{k}_{\pi/2}+\mathbf{q}}, \quad (34)$$

$$m_-(\mathbf{r})=\sqrt{2}\int\frac{d^3q}{(2\pi)^3}\exp(i\mathbf{q}\cdot\mathbf{r})\hat{m}_{-\mathbf{k}_{\pi/2}+\mathbf{q}},$$

where $m_-(\mathbf{r})$ is the complex conjugate of $m_+(\mathbf{r})$, one can express the free-energy functional in the following Ginzburg-Landau form:

$$\frac{F}{N}=\int d^3\mathbf{r}\left[\frac{1}{2}c\left|\left(\frac{\partial}{\partial x}-i\frac{a}{2c}\right)m_+\right|^2+\frac{1}{2}c'|\nabla_\perp m_+|^2\right.$$
$$\left.+\frac{1}{2}\left(r-\frac{a^2}{4c}\right)|m_+|^2+\frac{T}{8}|m_+|^4+\frac{T}{8}(m_+^4+m_-^4)\right], \quad (35)$$

where $\boldsymbol{\nabla}_\perp=(0,\partial/\partial y,\partial/\partial z)$ and the last term is generated by the umklapp terms. Following Bak and von Boehm [23], we choose the following ansatz for the order parameters:

$$m_\pm=A\exp[\pm i\phi(x)], \quad (36)$$

where the amplitude A is a constant. Note that $\phi(x)$ is constant in the commensurate $\langle 2\rangle$ phase and that A can be obtained by minimizing the free energy in that phase, which gives $A^2=3|r|/T$. Inserting the above expression in Eq. (35) leads, up to a constant, to the following free-energy functional per unit area perpendicular to the x direction:

$$F[\phi]=\frac{cA^2}{2}\int dx\left[\phi'^2(x)-\frac{a}{c}\phi'(x)-\frac{TA^2}{12c}[1-\cos 4\phi(x)]\right], \quad (37)$$

where the first term is minimized for $\phi(x)=Ax/(2c)$, which corresponds to an incommensurate spatial modulation, whereas the second term is minimized for $\phi(x)=0$, i.e., in the commensurate $\langle 2\rangle$ phase. The overall minimization of $F[\phi]$ is attained when the phase function $\phi(x)$ obeys the sine-Gordon equation:

$$\phi''(x)+4v\sin[4\phi(x)]=0, \quad (38)$$

where $v=TA^2/(24c)$. The solution consists of regions of constant phase separated by solitons in which ϕ increases by $\pi/2$ over a short distance. More generally, one can look for a solution over a (large) distance L that consists of n equally spaced solitons where $n\pi/2=L\phi'$. The corresponding free energy is given by [25,26]

$$\frac{F}{cA^2L}=\left[\frac{4}{\pi}v^{1/2}-\left|\frac{-a}{2c}\right|\right]\phi'+\frac{16}{\pi}v^{1/2}\phi'\exp\left(-\frac{2\pi}{\phi'}v^{1/2}\right), \quad (39)$$

where $\phi'=n\pi/(2L)$. The first term, proportional to the soliton density, is the formation energy; the second term corresponds to a weak repulsion between solitons. The commensurate phase is stable as long as the first term remains positive; otherwise, the $\langle 2\rangle$ phase becomes unstable with the respect to soliton formation. The critical temperature corresponding to this melting transition is given by

$$T_{\langle 2\rangle-IC}=4-2\pi Q+4\pi Q v(0)-\frac{\pi}{4}\frac{(1-\pi Q)^2}{Q}, \quad (40)$$

and is shown as a dashed line in Figs. 4 and 5.

A similar analysis can be performed to study, for instance, the stability of the $\langle 3\rangle$ phase near the critical line. The main changes are that the relevant ordering wave vector is now $(\pi/3,0,0)$ and that the sixth-order umklapp terms should be kept in Eq. (32). A transition between the $\langle 3\rangle$ phase and incommensurate phases is found for

$$T_{\langle 3\rangle-IC}=5-4\pi Q+4\pi Q v(0)-\frac{3\pi}{4}|1-4\pi Q|\sqrt{\frac{5(5-4\pi Q)}{1+20\pi Q}}. \quad (41)$$

The result is shown as dotted curves in Fig. 5. The deviation from the numerical solution of the mean-field equations that is seen when moving further away from the critical line comes from the truncation of the free-energy functional that is used in the soliton approach.

V. DISCUSSION

The fact that spin models with competing interactions can give rise to complex spatially modulated phases has been known for several decades. The ANNNI model is one of the simplest and best-studied such system, in which Ising spin variables situated on a lattice are coupled via nearest-neighbor ferromagnetic interactions in $(D-1)$-dimensional layers orthogonal to, say, the x axis and via next-nearest-neighbor antiferromagnetic interactions along the x axis [12]. The major additional ingredient that is present in the Coulomb frustrated Ising ferromagnet and not the previously studied models is the long-range nature of the competing antiferromagnetic interaction. It is then worth reviewing some of the differences between the phase behavior of the

three-dimensional Coulomb frustrated ferromagnet and that of the three-dimensional ANNNI and related models [27]. First, the long $1/r$ range of the frustrating interaction forbids ferromagnetic ordering for any nonzero value of the frustration parameter Q, and, as a result, there is no Lifshitz point [28] in the model. Second, there is no highly degenerate multiphase point at zero temperature; this is in contrast with the ANNNI model that possesses an infinitely degenerate multiphase point at zero temperature, a point from which springs an infinite number of distinct commensurate modulated phases [29]. Third, the phase diagram of the Coulomb frustrated Ising ferromagnet, as illustrated in Fig. 5, displays an infinite number of distinct flowers of complex spatially modulated phases that emerge from zero-temperature two-phase coexistence points, the extent of the flowers in the $T-Q$ phase diagram decreasing as the frustration parameter decreases.

The long range of the antiferromagnetic interaction in the Coulomb frustrated ferromagnet also brings about additional limitations on the mean-field approach. On general grounds, one can expect the mean-field description to reproduce the topology of the phase diagram correctly, but to become increasingly inaccurate as one approaches the transition line, both from below and from above, because it overlooks the role of fluctuations. In the present case, the fluctuations have a major effect on the transition line: as argued by Brazovskii [30] on the basis of a self-consistent Hartree treatment of a field-theoretical model with properties similar to that of Coulomb frustrated Ising ferromagnet,[3] and confirmed by Monte Carlo simulations [15], the fluctuations drive the order-disorder transition from second to first order. The mean-field approach is thus questionable in the vicinity of the transition line (which is why it may not be worth pursuing the search for devil's staircases as was done for the ANNNI model [23,32]). However, the main points reviewed above are not affected.

APPENDIX A: CALCULATION OF THE COULOMBIC ENERGY OF LAMELLAR PHASES IN REAL SPACE

The calculation of the ground-state energy due to the long-range Coulombic interaction can be performed as follows. For lamellar phases, the sum over the reciprocal vectors is performed along one direction. One then obtains the one-dimensional potential corresponding to the inverse lattice Laplacian [14],

$$W(i)=2\pi Q\frac{\exp(-\alpha|i|)-1}{\alpha}, \tag{A1}$$

where α is a convergence factor that will be taken to zero at the end of the calculation. The introduction of $\alpha>0$ in the calculation allows one to handle conditionally convergent sums. The average Coulombic energy per site of a cell $2m$ is given by

$$E_C=\frac{1}{4m}\sum_{N'=-\infty}^{+\infty}\sum_{i,j=1}^{2m}W(|i-j+2mN'|)S_iS_j, \tag{A2}$$

where N' is the index for labeling the right and left cells and i,j denote sites within the cell. The energy per site can be divided into two parts: the first one comes from the interaction between the spins within the cell and the second one comes from the interaction between a spin and its images in the other cells; this reads

$$E_C=E_1+E_2=\frac{1}{4m}\sum_{i,j=1}^{2m}W(|i-j|)S_iS_j + \frac{1}{4m}\sum_{N'\neq 0}\sum_{i,j=1}^{2m}W(|i-j+2mN'|)S_iS_j. \tag{A3}$$

By considering all contributions between pairs of sites within the cell, one gets for E_1

$$E_1=\frac{1}{2m}\left(m(W(0)-W(m))+\sum_{n=1}^{m-1}[2(m-n)-n]W(n) - \sum_{n=m+1}^{2m-1}[(2m-n)-n]W(n)\right). \tag{A4}$$

After some calculation, and taking the limit $\alpha\to 0$ at the end, one gets

$$E_1=Q\left(\frac{2\pi m^2}{3}+\frac{\pi}{3}\right). \tag{A5}$$

The sum over the right and the left cells can also be performed, and E_2 is then given by

$$E_2=\frac{\pi Q}{2m}\sum_{i,j=1}^{2m}\frac{e^{-\alpha(2m+i-j)}+e^{-\alpha(2m+j-i)}}{\alpha(1-e^{-\alpha 2m})}S_iS_j. \tag{A6}$$

By using the electro-neutrality condition ($\Sigma_i S_i=0$), and in the limit $\alpha\to 0$, one obtains E_2, which has a finite value:

$$E_2=\frac{\pi Q}{4m^2}\sum_{i,j}(i-j)^2S_iS_j=-\frac{\pi Q}{2m^2}\left|\sum_{i=1}^{2m}iS_i\right|^2=-\frac{\pi Q m^2}{2}. \tag{A7}$$

This gives for the Coulombic energy E_c

$$E_c=Q\left(\frac{\pi m^2}{6}+\frac{\pi}{3}\right). \tag{A8}$$

By subtracting the self-energy of the inverse lattice Laplacian potential to Eq. (A8), one exactly recovers Eq. (10).

APPENDIX B: GROUND-STATE ENERGY OF TUBULAR AND ORTHORHOMBIC PHASES

Let us calculate the energy per site for configurations whose phases are periodic with a orthorhombic cell ($m_1\times m_2\times m_3$). The short-range energy per spin is obtained as

[3]It is worth pointing out that the field-theoretical description of the symmetric diblock copolymer systems has also been shown to belong to the class of ''Brazovskii'' Hamiltonians [13,22,31].

$$E_{SR} = -J\left(3 - \frac{2}{m_1} - \frac{2}{m_2} - \frac{2}{m_3}\right). \tag{B1}$$

In the reciprocal space, the allowed wave vectors have components $[(2n_1+1)\pi/m_1,(2n_2+1)\pi/m_2,(2n_3+1)\pi/m_3]$, with $0 \leqslant n_1 < m_1 - 1$, $0 \leqslant n_2 < m_2 - 1$, $0 \leqslant n_3 < m_3 - 1$, so that the Coulombic energy per spin E_c is given by

$$E_c = Q\left[\sum_{n_1=0}^{m_1-1}\sum_{n_2=0}^{m_2-1}\sum_{n_3=0}^{m_3-1}\left(\frac{\pi}{\left[\sum_{\alpha=1}^{3}\sin\left(\frac{(2n_\alpha+1)\pi}{2m_\alpha}\right)^2\right]\prod_{\alpha=1}^{3}\sin\left(\frac{(2n_\alpha+1)\pi}{2m_\alpha}\right)^2}\right) - 2\pi v(0)\right]. \tag{B2}$$

When both m_2 and m_3 go to infinity, one obtains lamellar phases of period $2m$, and Eq. (B2) reduces to Eq. (10).

When the periodic structure loses translational invariance in a second direction, one obtains a lattice of tubes whose perpendicular section is a rectangular cell $m_1 \times m_2$. Although we have not obtained a fully analytical expression for such phases, some results can be derived. The Coulombic energy for tubes of section $m_1 \times m_2$ is bounded as follows:

$$E_c(\inf(m_1,m_2)) \leqslant E_c(m_1,m_2) \leqslant E_c(\sup(m_1,m_2)). \tag{B3}$$

If $p \times m_1 = m_2 = m$, where p is a positive integer, the energy $E_c(m)$ behaves as

$$E_c(m^2) \simeq C(p)m^2 + O(m), \tag{B4}$$

where the numerical coefficients $C(p)$ are summarized in Table I.

We have also calculated numerically, via Eqs. (B1) and (B2) the total energy of modulated orthorhombic phases $(m_1 \times m_2 \times m_3)$ when $\infty > m_1, m_2, m_3 > 1$. It is always higher than that of the phases $(1 \times m_2 \times m_3)$ or $(1 \times 1 \times m_3)$.

APPENDIX C: MIXED LAMELLAR PHASES

The inverse Laplacian approximation allows one to calculate exactly the energy of a large number of periodic structures at zero temperature. As an illustration we present here the results for mixed lamellar phases that are potential ground-state candidates in the region of Q/J where the most stable among the simple lamellar phases involve lamellae of width $m=1$ (phase $\langle 1 \rangle$) and $m=2$ (phase $\langle 2 \rangle$).

TABLE I. Coefficient of the leading term of the Coulombic energy per site for periodic tubular structures $p = 1,2,3,5,\infty$.

p	$C(p)$	$C(p)*p^2$
1	0.222 08	0.222 08
2	0.089 083	0.356 33
3	0.045 957	0.413 61
4	0.027 568	0.441 09
5	0.018 304	0.457 6
∞	0	$\pi/6 = 0.523\,59\ldots$

1. The $\langle 1^n 2^p \rangle$ phases

The $\langle 1^n 2^p \rangle$ phases are the simplest mixed phases that one can construct with the two elementary bricks formed by lamellae of width $m=1$ and $m=2$: they are formed by a periodic sequence of ferromagnetically aligned layers whose fundamental period consists of n one-layer lamellae followed by p two-layer lamellae, two successive lamellae being formed by spins of opposite signs. Because of the electroneutrality (zero magnetization) condition, one has to distinguish three different families: $(n=2q, p=2r)$, $(n=2q+1, p=2r)$, and $(n=2q, p=2r+1)$, where q and r are integers. The $\langle 1^{2q+1}2^{2r+1} \rangle$ phases are not allowed at zero temperature because they it does not satisfy the electroneutrality condition. Because of the two-dimensional in-layer ferromagnetic ordering, the wave vectors characterizing lamellar phases have only one nonzero component.

a. The $\langle 1^{2q}2^{2r} \rangle$ phases

The size of the one-dimensional unit cell is $L = 2q + 4r$ and the allowed values of the nonzero components of the wave vector are $k = 2\pi l/(2q+4r)$ where l is an integer such that $l = 0, \ldots, 2q+4r-1$. Summing over all sites of the lattice, one finds

$$|\hat{S}(k)| = \frac{\sqrt{N}}{2q+4r}\frac{|\sin(2rk)|}{\left|\cos(k)\cos\left(\frac{k}{2}\right)\right|} = \frac{\sqrt{N}}{2q+4r}\frac{|\sin(qk)|}{\left|\cos(k)\cos\left(\frac{k}{2}\right)\right|}, \tag{C1}$$

if $k \neq \pm\pi/2$ and $k \neq \pi$. Otherwise, one obtains $|\hat{S}(\pm\pi/2)| = [\sqrt{N}/(2q+4r)]\sqrt{8}r$ and $|\hat{S}(\pi)| = [\sqrt{N}/(2q+4r)]2q$.

Using the identities

$$\sum_{l=1}^{q+2r-1}\frac{\sin\left(\frac{q\pi l}{q+2r}\right)^2}{\cos\left(\frac{\pi l}{q+2r}\right)^2\cos\left(\frac{\pi l}{2(q+2r)}\right)^2} = 8r(r+q) \tag{C2}$$

and

$$\sum_{l=1}^{q+2r-1} \frac{\sin\left(\frac{q\pi l}{q+2r}\right)^2}{\sin\left(\frac{2\pi l}{q+2r}\right)^2} = r(r+q), \tag{C3}$$

one can express the Coulombic energy per spin as

$$E_c = Q\left[\pi \frac{2q^2+16r^2+16qr}{(2q+4r)^2} - 2\pi v(0)\right]. \tag{C4}$$

The short-range contribution can be easily calculated and the total energy per spin is equal to

$$E_{\langle 1^{2q}2^{2r}\rangle} = J\left(-2+\frac{q}{q+2r}\right) + Q\left(\pi \frac{2q^2+16r^2+16qr}{(2q+4r)^2} - 2\pi v(0)\right). \tag{C5}$$

It is now easy to show that the above energy, whatever the strictly positive values of q and r and whatever the value of Q/J, cannot be less than either the energy of the $\langle 1\rangle$ phase or that of the $\langle 2\rangle$ phase. Indeed, for the conditions $E_{\langle 1^{2q}2^{2r}\rangle} \leqslant E_{\langle 1\rangle}$ and $E_{\langle 1^{2q}2^{2r}\rangle} \leqslant E_{\langle 2\rangle}$ to be simultaneously satisfied, one must have

$$\frac{2q+4r}{\pi q} \leqslant Q/J \leqslant \frac{q+2r}{\pi(q+r)}, \tag{C6}$$

which is impossible.

b. The $\langle 1^{2q+1}\rangle$ and $\langle 1^{2q}2^{2r+1}\rangle$ phases

To satisfy the requirement of the global electroneutrality, the unit cell of such phases is built as follows. For the $\langle 1^n 2^{2r}\rangle$ phases, with $m=2q+1$, the unit cell is

$$\underbrace{\uparrow\downarrow\uparrow\downarrow\ldots\uparrow}_{n}\ \underbrace{\downarrow\downarrow\uparrow\uparrow\ldots\downarrow\downarrow\uparrow\uparrow}_{2r}\ \underbrace{\downarrow\uparrow\downarrow\ldots\downarrow}_{n}\ \underbrace{\uparrow\uparrow\downarrow\downarrow\ldots\uparrow\uparrow\downarrow\downarrow}_{2r}$$

and the nonzero components of the wave vector are given by $k=2\pi l/(8r+2n)$ where $l=1\ldots 8r+2n-1$. After some algebra, the Fourier transform of the spin variable $\hat{S}(k)$ is obtained as

$$|\hat{S}(k)| = \frac{\sqrt{N}}{2n+8r} \frac{2\left|\cos\left(\frac{nk}{2}\right)\right|}{\left|\cos(k)\cos\left(\frac{k}{2}\right)\right|} \tag{C7}$$

if $k\neq\pi$ and $|\hat{S}(\pi)| = [\sqrt{N}/(2n+8r)]2n$. The total energy per spin is then

$$E_{\langle 1^n 2^{2r}\rangle} = J\left(-2+\frac{2n}{2n+8r}\right) + Q\left(\pi \frac{2n^2+64r^2+32rn}{(2n+8r)^2} - 2\pi v(0)\right). \tag{C8}$$

The $\langle 1^{2q}2^m\rangle$ phase with $m=2r+1$ is characterized by the sequence

$$\underbrace{\uparrow\downarrow\uparrow\downarrow\ldots\uparrow\downarrow}_{2q}\ \underbrace{\uparrow\uparrow\downarrow\downarrow\ldots\downarrow\downarrow\uparrow\uparrow}_{m}\ \underbrace{\downarrow\uparrow\ldots\downarrow\uparrow}_{2q}\ \underbrace{\downarrow\downarrow\ldots\uparrow\uparrow\downarrow\downarrow}_{m}$$

and the nonzero components of the wave vector are given by $k=2\pi l/(4m+4q)$ with $l=1\ldots 4m+4q-1$. This leads to

$$|\hat{S}(k)| = \frac{\sqrt{N}}{4q+4m} \frac{2|\sin(qk)|}{\left|\cos(k)\cos\left(\frac{k}{2}\right)\right|} \tag{C9}$$

if $k\neq\pm\pi/2$, and $|\hat{S}(\pm\pi/2)| = \sqrt{N}/(4q+4m)2\sqrt{2}q$. The total energy per spin is finally given by

$$E_{\langle 1^{2q}2^m\rangle} = J\left(-2+\frac{q}{q+m}\right) + Q\left(\pi \frac{32q^2+64m^2+32mq}{(4q+4m)^2} - 2\pi v(0)\right). \tag{C10}$$

As before, there is no range of the frustration parameter Q/J for which these phases become ground states of the system.

2. Energy of defects in the $\langle 2\rangle$ phase

The issue of the stability of the mixed versus simple lamellar phases can be addressed in a different way. Starting from the $\langle 2\rangle$ phase, one can calculate the energy change brought by inserting one or several defects of type $\langle 1\rangle$ within the periodic structure. The creation of one such defect results from the flip of a pair of up-down spins. This corresponds to the simplest excitation that one expects in the $\langle 2\rangle$ phase: $\ldots\uparrow\uparrow\downarrow\downarrow\uparrow\uparrow\downarrow\downarrow\ldots \Rightarrow \ldots\uparrow\uparrow\downarrow\uparrow\downarrow\uparrow\downarrow\downarrow\ldots$ The resulting defective structure can also be viewed as a $\langle 1^4 2^{2m}\rangle$ phase where $m\to\infty$. The Coulombic energy of a $\langle 1^4 2^{2m}\rangle$ structure for a cell of size $4+4m$ is derived from Eq. (C4) and reads

$$e_{c\langle 1^4 2^{2m}\rangle} = (4+4m)E_{c\langle 1^4 2^{2m}\rangle} = Q\left[\pi \frac{2+4m^2+8m}{1+m} - 2\pi v(0)(4+4m)\right]. \tag{C11}$$

If one subtracts the Coulombic energy of the $\langle 2\rangle$ phase for the same unit cell ($l=4+4m$) from the above equation, one obtains the Coulombic energy for one excitation in a $\langle 2\rangle$ phase. Strikingly, this energy goes to zero when m goes to infinity, which means that the presence of one defect in the $\langle 2\rangle$ phase does not change at all the Coulombic energy of this phase. (This is not a result of the macroscopic limit.)

Conversely, this defect has a short-range energy cost that is easily obtained as $E_{SR}=4$. In all the region of frustration parameters Q/J where the $\langle 2\rangle$ phase is more stable than any other simple lamellar phase, the presence of one defect is then energetically unfavorable for the system.

We have also calculated the energy of a $\langle 2\rangle$ phase where two defects have been introduced. We have first calculated the energy of the $\langle 2^{2m}1^{2p}2^{2n}1^{2q}\rangle$ and $\langle 2^{2m+2n}1^{2p+2q}\rangle$ phases that are identical. Setting $p=q=2$, whereas $n,m\rightarrow\infty$, one obtains the energy of the $\langle 2\rangle$ phase in the presence of two defects. We have also found that the introduction of the two defects is energetically unfavorable for the system for any value of the frustration. Although we have not obtained a general proof, the phase-locking into simple lamellar phases at zero temperature seems to be well established for the model.

[1] F. Bates and G. Fredrickson, Annu. Rev. Phys. Chem. **41**, 525 (1990).
[2] M.W. Matsen and F.S. Bates, Macromolecules **29**, 1091 (1996).
[3] D. Wu, D. Chandler, and B. Smit, J. Phys. Chem. **96**, 4077 (1992).
[4] M.W. Deem and D. Chandler, Phys. Rev. E **49**, 4268 (1994).
[5] H.J. Woo, C. Carraro, and D. Chandler, Phys. Rev. E **52**, 6497 (1995).
[6] T. Garel and S. Doniach, Phys. Rev. B **26**, 325 (1982).
[7] E.W. Carlson, S.A. Kivelson, Z. Nussinov, and V.J. Emery, Phys. Rev. B **57**, 14 704 (1998).
[8] D. Kivelson, G. Tarjus, and S.A. Kivelson, Prog. Theor. Phys. **126**, 289 (1996).
[9] C. Carraro, Physica A **236**, 130 (1997).
[10] R. Elliot, Phys. Rev. **124**, 346 (1961).
[11] W. Selke and M.E. Fisher, Phys. Rev. B **20**, 257 (1979).
[12] W. Selke, Phys. Rep. **170**, 213 (1988).
[13] T. Ohta and K. Kawazaki, Macromolecules **19**, 2621 (1986).
[14] H. Kleinert, *Gauge Fields in Condensed Matter* (World Scientific, Singapore, 1989).
[15] P. Viot and G. Tarjus, Europhys. Lett. **44**, 423 (1998).
[16] Z. Nussinov, J. Rudnick, S.A. Kivelson, and L.N. Chayes, Phys. Rev. Lett. **83**, 472 (1999).
[17] L. Chayes, V.J. Emery, S.A. Kivelson, Z. Nussinov, and G. Tarjus, Physica A **225**, 129 (1996).
[18] A.B. MacIsaac, J.P. Whitehead, M.C. Robinson, and K. De'Bell, Phys. Rev. B **51**, 16 033 (1995).
[19] U. Low, V.J. Emery, K. Fabricius, and S.A. Kivelson, Phys. Rev. Lett. **72**, 1918 (1994).
[20] D. Frenkel and B. Smit, *Understanding Molecular Simulation: From Algorithms to Applications* (Academic, London, 1996).
[21] J. Luck, C. Godrèche, A. Janner, and T. Jansen, J. Phys. A **26**, 1951 (1993).
[22] L. Leibler, Macromolecules **13**, 1602 (1980).
[23] P. Bak and J. von Boehm, Phys. Rev. B **21**, 5297 (1980).
[24] M.H. Jensen and P. Bak, Phys. Rev. B **29**, 6280 (1984).
[25] P. Bak and V. Emery, Phys. Rev. Lett. **36**, 978 (1976).
[26] J.K. Perring and T.H.R. Skyrme, Nucl. Phys. **31**, 550 (1962).
[27] P. Upton and J. Yeomans, Phys. Rev. B **40**, 479 (1989).
[28] R.M. Hornreich, M. Luban, and S. Shtrikman, Phys. Rev. Lett. **35**, 1678 (1975).
[29] P.M. Duxbury and W. Selke, J. Phys. A **16**, L741 (1983).
[30] S.A. Brazovskii, Sov. Phys. JETP **41**, 85 (1975).
[31] G.H. Fredrickson and E. Helfand, J. Chem. Phys. **87**, 697 (1987).
[32] P. Bak and R. Bruinsma, Phys. Rev. Lett. **49**, 249 (1982).